UKAEA-CCFE-PR(21)54

Pui-Wai Ma, Sergei L. Dudarev

Elastic dipole tensor of a defect: finite temperature definition and properties

Enquiries about copyright and reproduction should in the first instance be addressed to the UKAEA Publications Officer, Culham Science Centre, Building K1/0/83 Abingdon, Oxfordshire, OX14 3DB, UK. The United Kingdom Atomic Energy Authority is the copyright holder.

The contents of this document and all other UKAEA Preprints, Reports and Conference Papers are available to view online free at scientific-publications.ukaea.uk/

Elastic dipole tensor of a defect: finite temperature definition and properties

Pui-Wai Ma, Sergei L. Dudarev

This is a preprint of a paper submitted for publication in
Physical Review Materials

Elastic dipole tensor of a defect: finite temperature definition and properties

Pui-Wai Ma* and S. L. Dudarev
UK Atomic Energy Authority, Culham Science Centre, Oxfordshire, OX14 3DB, United Kingdom

The concept of elastic dipole tensor of a defect is generalised to enable the treatment of lattice distortions produced by defects at elevated temperatures. Thermodynamic and statistical mechanics treatments show the feasibility of applying the formalism to the evaluation of formation free energies and finite-temperature elastic dipole tensors of $\frac{1}{2}\langle 111\rangle$ prismatic self-interstitial atom dislocation loops. The method exhibits good numerical stability even in the high temperature limit, and relates discrete atomic and continuum representations of displacement and stress fields of defects.

I. INTRODUCTION

In a crystalline material, defects form naturally by thermal excitation. At a thermal equilibrium, the concentration of defects is determined by their formation free energy and temperature. High concentration of defects, far exceeding the equilibrium value, can also be produced by mechanical deformation or by exposing the material to a flux of energetic particles [1–4].

There is an extensive variety of types of defects. Some of them can be readily classified and identified as a vacancy, a self-interstitial atom, a dislocation loop, a void, or an extended dislocation. Defects evolve under the effect of applied stress and temperature, segregating and agglomerating as a result of elastic interactions [5, 6], or annihilate in reactions involving defects of opposite type. Evolution of microstructure driven by the generation of defects and reactions between them alters mechanical and physical properties of materials [7].

Defects distort the surrounding crystal lattice, producing spatially varying strain and stress fields. The strain field of a localized defect can be computed from its elastic dipole tensor and elastic Green's function [8–17], where the dipole tensor is a fundamental quantity fully defining the elastic properties of a defect in the asymptotic far-field limit [18]. Elements of the relaxation volume tensor and volumes of defects can also be computed using atomistic or *ab initio* methods [10–17, 19, 20].

The notion of elastic dipole tensor effectively transfers information, derived from discrete atomic configurations, to the continuum limit, and enables treating defects as objects of elasticity theory. This provides a foundation for the continuum models of microstructural evolution and enables the evaluation of stress and strain fields on the spatial scale many orders of magnitude larger than that accessible to atomistic or electronic scale models [5, 6, 21].

The energy of elastic interaction between a defect and an external strain field ϵ_{ij}^{ext} can be written as

$$\mathcal{E}_{int}^{ext} = -P_{ij}\epsilon_{ij}^{ext}, \tag{1}$$

whereas the energy of elastic interaction between any two defects separated by a distance many times their size is

$$\mathcal{E}_{int}^{ab} = P_{ij}^{a}P_{kl}^{b}\frac{\partial^2}{\partial x_j \partial x_l}G_{ik}(\mathbf{r}), \tag{2}$$

where P_{ij}^{a} and P_{kl}^{b} are the dipole tensors of defects a and b, $\mathbf{r}$ is the relative position vector of the defects, and G_{ik} is the elastic Green's function. G_{ik} can be evaluated numerically for an arbitrary elastically anisotropic material [22] from its elastic constants tensor C_{ijkl}.

The pairwise nature of elastic interactions makes equations (1) and (2) easy and convenient for implementing in coarse-grained models, for example object kinetic Monte Carlo (kMC) [23–25] or defect dynamics [21]. Using the dipole tensor formalism, Sivak *et al.* estimated the effect of elastic interactions on the diffusion of defects in bcc iron and vanadium [23], as well as on the diffusion of hydrogen in bcc iron [24, 25]. Baraglia *et al.* [21] used equations (1) and (2) in simulations of time evolution of an ensemble of dislocation loops in tungsten.

A point that so far has not been extensively studied in the context of models using elastic dipole tensor formalism, is the temperature effect. All the calculations of dipole tensors of defects [14–16] were performed, and results were applied without considering thermal effects, despite the fact that applications always refer to observations or simulations assuming finite temperature dynamics [21, 23–25]. For example, it is the energy rather than the free energy that is used in the analysis, and all the calculations of dipole tensors were performed using molecular statics or density function theory involving direct energy minimization *via* ionic relaxation [14–17].

In this study, we extend the notion of elastic dipole tensor to finite temperatures. We derive it from both the thermodynamics (macroscopic) and statistical mechanics (microscopic) perspectives using the free energy as the central notion of the theory of elasticity [26]. We find that the derivation leads to the same consistent result provided that the Cauchy stress is taken as being equivalent to the ensemble average of virial stress. We discuss the numerical procedure for calculating the formation free energy and elastic dipole tensor of defects, considering $\frac{1}{2}\langle 111\rangle$ self-interstitial atom (SIA) loops in tungsten as examples.

---

* leo.ma@ukaea.uk

II. THEORY

At a finite temperature, the quantity that is used for evaluating thermodynamic properties of a material is its free energy as opposed to energy. The free energy of an elastically strained crystalline solid equals [26]

$$\mathcal{F} = \frac{1}{2}\int \sigma_{ij}(\mathbf{r})\epsilon_{ij}(\mathbf{r})dV, \tag{3}$$

where σ_{ij} and ϵ_{ij} are the internal stress and strain, respectively. If the elastic stress and strain fields in the above equation are generated by the presence of a defect, the integral above gives its elastic free self-energy.

A small variation of the elastic field gives rise to a small variation in the free energy

$$\begin{aligned}\mathcal{F}+\delta\mathcal{F} &= \frac{1}{2}\int \sigma_{ij}(\mathbf{r})\epsilon_{ij}(\mathbf{r})dV + \int \sigma_{ij}(\mathbf{r})\delta\epsilon_{ij}(\mathbf{r})dV \\ &= \frac{1}{2}\int \sigma_{ij}(\mathbf{r})\epsilon_{ij}(\mathbf{r})dV + \int \epsilon_{ij}(\mathbf{r})\delta\sigma_{ij}(\mathbf{r})dV, \end{aligned}\tag{4}$$

where the equivalence of the two expressions in (4) stems from the quadratic form of (3) and the fact that $\sigma_{ij}(\mathbf{r}) = C_{ijkl}\epsilon_{kl}(\mathbf{r})$.

If the variation of strain is spatially homogeneous $\delta\epsilon_{ij}(\mathbf{r}) = \delta\epsilon_{ij}$, we write

$$\mathcal{F}(\delta\epsilon_{ij}) = \mathcal{F}(\delta\epsilon_{ij}=0) + \left.\frac{\partial\mathcal{F}}{\partial\epsilon_{ij}}\right|_{\delta\epsilon_{ij}=0}\delta\epsilon_{ij}, \tag{5}$$

and hence

$$\mathcal{F}(\delta\epsilon_{ij}) = \mathcal{F}(\delta\epsilon_{ij}=0) + \int \sigma_{ij}(\mathbf{r})dV\delta\epsilon_{ij}. \tag{6}$$

Differentiating the above equation with respect to strain, we find the dipole tensor of the defect, expressed as a volume integral of its stress field [10, 11, 18]

$$P_{ij} = \frac{\partial\mathcal{F}}{\partial\epsilon_{ij}} = \int \sigma_{ij}(\mathbf{r})dV. \tag{7}$$

The stress field here refers to its finite temperature value [26]. Similarly, by differentiating the free energy with respect to a spatially homogeneous stress, we find the relaxation volume tensor of the defect [13, 27] expressed as a volume integral of its strain field

$$\Omega_{ij} = \frac{\partial\mathcal{F}}{\partial\sigma_{ij}} = \int \epsilon_{ij}(\mathbf{r})dV. \tag{8}$$

The two quantities (7) and (8) are related by the equation $P_{ij} = C_{ijkl}\Omega_{kl}$.

The free energy of interaction between a defect and a spatially homogeneous or slowly varying external field can now be readily derived from (4) using the fact that in equilibrium the variation of the stress field of the defect equals the applied external stress field taken with the opposite sign [18, 26, 28]

$$\mathcal{F}_{int}^{ext} = -\Omega_{ij}\sigma_{ij}^{ext} = -P_{ij}\epsilon_{ij}^{ext}. \tag{9}$$

In statistical mechanics, the free energy is related to the the partition function of the system as

$$\mathcal{F} = -k_B T \ln \mathcal{Z}. \tag{10}$$

The partition function is

$$\mathcal{Z} = \int \exp(-\beta\mathcal{H})d\Omega, \tag{11}$$

where $\beta = (k_B T)^{-1}$ and $d\Omega$ is an element of phase space volume. Taking a functional derivative of the free energy with respect to the internal strain gives

$$\frac{\delta\mathcal{F}}{\delta\epsilon_{ij}} = \frac{1}{\mathcal{Z}}\int \exp(-\beta\mathcal{H})\frac{\delta\mathcal{H}}{\delta\epsilon_{ij}}d\Omega = \left\langle \frac{\delta\mathcal{H}}{\delta\epsilon_{ij}} \right\rangle, \tag{12}$$

where brackets $\langle ... \rangle$ refer to an ensemble average.

For an atomic system subjected to a small spatially homogeneous external strain, the atomic position vectors transform in response to strain as

$$\mathbf{r} \to (\mathbf{I} + \boldsymbol{\epsilon}^{ext})\mathbf{r}. \tag{13}$$

Similarly, the momenta of atoms transform as

$$\mathbf{p} \to (\mathbf{I} + \boldsymbol{\epsilon}^{ext})^{-1}\mathbf{p}. \tag{14}$$

The above scaling of momentum is consistent with the definition of the momentum operator $\hat{\mathbf{p}} = -i\hbar\partial/\partial\mathbf{r}$ in quantum mechanics [29] or in the Lagrangian classical mechanics [30], where the momentum is defined as a derivative of the Lagrangian function with respect to the corresponding velocity $p_i = \partial\mathcal{L}/\partial\dot{q}_i$. This results in

$$\left(\frac{\delta r_{n\alpha}}{\delta\epsilon_{ij}^{ext}}\right)_{\epsilon_{ij}^{ext}=0} = r_{nj}\delta_{\alpha i}, \tag{15}$$

$$\left(\frac{\delta p_{n\alpha}}{\delta\epsilon_{ij}^{ext}}\right)_{\epsilon_{ij}^{ext}=0} = -p_{nj}\delta_{\alpha i}. \tag{16}$$

Consider a generic atomic scale Hamiltonian of the form

$$\mathcal{H} = \sum_n \frac{\mathbf{p}_n^2}{2m} + U(\{\mathbf{r}\}). \tag{17}$$

where U is the potential energy, the value of which is uniquely defined from an atomic configuration $\{\mathbf{r}\}$. The functional derivative of the Hamiltonian with respect to an external strain is

$$\begin{aligned}\frac{\delta\mathcal{H}}{\delta\epsilon_{ij}^{ext}} &= \sum_{n,\alpha}\frac{p_{n\alpha}}{m}\left(\frac{\delta p_{n\alpha}}{\delta\epsilon_{ij}^{ext}}\right) + \sum_{n,\alpha}\frac{\partial U}{\partial r_{n\alpha}}\left(\frac{\delta r_{n\alpha}}{\delta\epsilon_{ij}^{ext}}\right) && (18)\\ &= -\sum_n \frac{p_{ni}p_{nj}}{m} - \sum_n F_{ni}r_{nj} && (19)\\ &= -\sum_n \frac{p_{ni}p_{nj}}{m} + \frac{1}{2}\sum_{nm} F_{nmi}(r_{mj}-r_{nj}) && (20)\\ &= \sum_n \Omega_n\sigma_{nij}^{vir} && (21)\end{aligned}$$

where $F_{ni} = -\partial U/\partial r_{ni}$ is the i-th Cartesian component of the force acting on atom n, and F_{nmi} is the i-th component of force acting on atom n due to its interaction with atom m. The virial stress on atom n is defined as [31, 32],

$$\sigma^{vir}_{nij} = \frac{1}{\Omega_n}\left(-\frac{p_{ni}p_{nj}}{m} + \frac{1}{2}\sum_m F_{nmi}(r_{mj} - r_{nj})\right) \quad (22)$$

where Ω_n is the volume of atom n, defined for example using the Voronoi partitioning of the lattice. The sign convention for the virial stress is that $P = -\frac{1}{3}\mathrm{Tr}(\bar{\boldsymbol{\sigma}}^{vir})$, where P is the external hydrostatic pressure. In equilibrium, the virial stress has the sign opposite to the sign of the internal stress. Therefore, we write

$$\frac{\delta\mathcal{H}}{\delta\epsilon_{ij}} = -\frac{\delta\mathcal{H}}{\delta\epsilon^{ext}_{ij}} = -\sum_n \Omega_n\sigma^{vir}_{nij} = \sum_n \Omega_n\sigma_{nij}, \quad (23)$$

where σ_{nij} is the internal stress. Finally, we arrive at (cf. equation (7))

$$\frac{\delta\mathcal{F}}{\delta\epsilon_{ij}} = \left\langle\frac{\delta\mathcal{H}}{\delta\epsilon_{ij}}\right\rangle = \left\langle\sum_n \Omega_n\sigma_{nij}\right\rangle \approx \left\langle\int\sigma_{ij}dV\right\rangle = V\langle\bar{\sigma}_{ij}\rangle \quad (24)$$

where $\bar{\sigma}_{ij}$ is the macrostress, which is the same as average macroscopic stress. The last equality holds following the same argument as that given in Ref. [13], where a defect in a finite size simulation cell is treated using the periodic boundary conditions. The elastic dipole tensor, derived using a microscopic argument, can now be written as

$$P_{ij} = \left\langle\int\sigma_{ij}dV\right\rangle. \quad (25)$$

This expression has the form similar to that derived from the energy argument at 0K [10–17], however now the formula also includes taking the ensemble average. Furthermore, we find that the expression for the elastic dipole tensor in the macroscopic thermodynamics (7) is equivalent to that derived from the microscopic statistical mechanics, provided that the Cauchy stress is taken as equivalent to the ensemble average value of the virial stress.

III. UMBRELLA SAMPLING

The non-stationary nature of a defect presents a difficulty in the context of evaluation of its thermodynamic properties, since a defect migrates and evolves due to the effect of thermal fluctuations. We circumvent this problem using a biased sampling technique known as the umbrella sampling [33]. It is a re-weighting technique for evaluating a thermodynamic quantity of a target state by sampling a reference state. We briefly outline the method here, and then apply it specifically to the case of a defect at a finite temperature. We note that the method only applies in the classical limit, and it does not treat the low temperature case where quantum-mechanical effects dominate the properties and dynamics of defects [34, 35].

We consider two classical Hamiltonians $\mathcal{H}^0$ and $\mathcal{H}^1$, and their difference:

$$\delta\mathcal{H}_{um} = \mathcal{H}^1 - \mathcal{H}^0. \quad (26)$$

The ensemble average of an observable $\mathcal{O}$ with respect to Hamiltonian $\mathcal{H}^0$ at temperature T is

$$\langle\mathcal{O}\rangle_0 = \frac{\int\mathcal{O}\exp(-\beta\mathcal{H}^0)d\Omega}{\int\exp(-\beta\mathcal{H}^0)d\Omega}. \quad (27)$$

Substituting (26) into (27), we find

$$\langle\mathcal{O}\rangle_0 = \frac{\langle\mathcal{O}\exp(\beta\delta\mathcal{H}_{um})\rangle_1}{\langle\exp(\beta\delta\mathcal{H}_{um})\rangle_1}. \quad (28)$$

This formula replaces a calculation of an average of an observable $\mathcal{O}$ over an ensemble defined by Hamiltonian $\mathcal{H}^0$ by calculations of averages of $\mathcal{O}\exp(\beta\delta\mathcal{H}_{um})$ and $\exp(\beta\delta\mathcal{H}_{um})$ over an ensemble defined by another Hamiltonian $\mathcal{H}^1$.

We apply the above formula to the calculation of elastic dipole tensor of a defect. The functional derivative of the free energy of a system defined by Hamitonian $\mathcal{H}^0$ is

$$\frac{\delta\mathcal{F}^0}{\delta\epsilon_{ij}} = \frac{1}{\mathcal{Z}^0}\int\exp(-\beta\mathcal{H}^0)\frac{\delta\mathcal{H}^0}{\delta\epsilon_{ij}}d\Omega. \quad (29)$$

Using (26)-(28), we transform this equation into

$$\frac{\delta\mathcal{F}^0}{\delta\epsilon_{ij}} = \frac{\left\langle\frac{\delta\mathcal{H}^0}{\delta\epsilon_{ij}}\exp(\beta\delta\mathcal{H}_{um})\right\rangle_1}{\langle\exp(\beta\delta\mathcal{H}_{um})\rangle_1}. \quad (30)$$

The right-hand side of this equation is consistent with Eq. (28), showing that the derivative of the free energy and hence the dipole tensor of a defect can be evaluated using the umbrella sampling approach.

The free energy corresponding to Hamiltonian $\mathcal{H}^0$ can be written as

$$\begin{aligned}\mathcal{F}^0 &= -k_BT\ln Z^0 && (31)\\ &= -k_BT\ln\int\exp(-\beta\mathcal{H}^0)d\Omega && (32)\\ &= -k_BT\ln\int\exp(\beta\delta\mathcal{H}_{um})\exp(-\beta\mathcal{H}^1)d\Omega && (33)\\ &= -k_BT\ln\langle\exp(\beta\delta\mathcal{H}_{um})\rangle_1 + \mathcal{F}^1. && (34)\end{aligned}$$

Hence, the free energy $\mathcal{F}^0$ can be evaluated using sampling over the ensemble defined by Hamiltonian $\mathcal{H}^1$ if $\mathcal{F}^1$ is known.

In practice, assuming that the system of interest involves N atoms, we choose Hamiltonian $\mathcal{H}^1$ as a sum of N three-dimensional harmonic oscillators

$$\mathcal{H}^1 = \mathcal{H}_{HO} = \sum_n\left(\frac{\mathbf{p}_n^2}{2m} + \frac{1}{2}m\omega^2\mathbf{x}_n^2 + C\right), \quad (35)$$

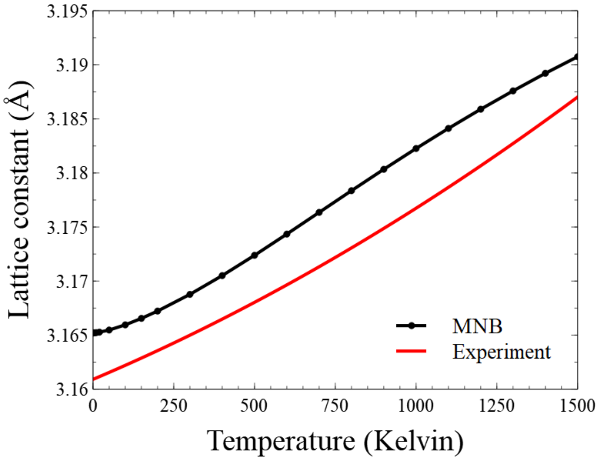

FIG. 1. Equilibrium lattice constants, calculated using the Mason-NguyenManh-Becquart (MNB) [39] tungsten interatomic potential over a range of elevated temperatures. Experimental curve is given by a fitted formula taken from Ref. [40], where the measurements span the range from 25 to 900°C.

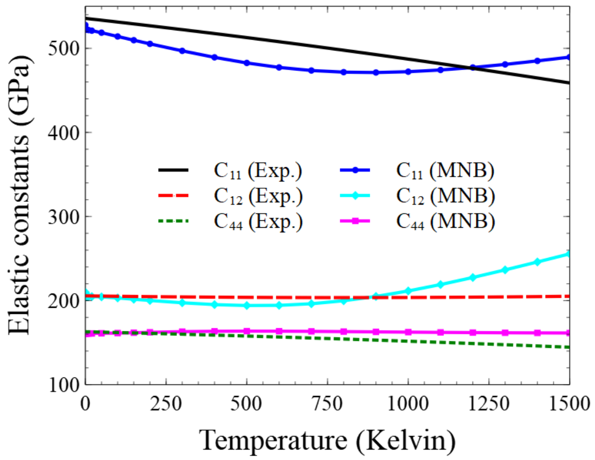

FIG. 2. Elastic constants C_{11}, C_{12}, and C_{44} evaluated from the free energy computed using the MNB potential for tungsten. Experimental data are taken from Ref. [41], where the measurements span the temperature range up to 1800°C.

where $\mathbf{x}_n = \mathbf{r}_n - \mathbf{R}_n$ is the coordinate of an oscillator, defined near an equilibrium atomic position $\mathbf{R}_n$, ω is its frequency and m its mass, and C is a constant. The free energy of this system of oscillators can be evaluated analytically as [36]

$$\mathcal{F}^1 = \mathcal{F}_{HO} = -3Nk_BT \ln\left(\frac{k_BT}{\hbar\omega}\right) + NC, \tag{36}$$

where the Planck constant is included for dimensional convenience. In what follows, we assume that ω equals the Debye frequency of tungsten, $\hbar\omega = k_BT_D$, where $T_D = 400$K. Constant C is adjusted on-the-fly during the thermalization of a system, but remains fixed during sampling in order to minimize $\delta\mathcal{H}_{um}$ and achieve higher accuracy of the final result. The initial atomic configuration containing a defect $\{\mathbf{R}_n\}$ is determined through energy minimization *via* atomic relaxation performed using the conjugate gradient method. The actual sampling is performed using molecular dynamic simulations, integrating the corresponding Langevin equations of motion [37].

IV. SIMULATIONS

Simulations exploring the finite temperature properties of defects were performed for $\frac{1}{2}\langle 111\rangle$ SIA loops of different size in tungsten. We computed the formation free energies and elastic dipole tensors of loops at finite temperatures. All the simulations were performed using the SPILADY code [38] modified to include the analysis carried out in this study.

The initial analysis was performed using simulation cells containing $30 \times 30 \times 30$ BCC unit cells and 54,000 atoms. We used the Mason-Nguyen-Manh-Becquart (MNB) [39] interatomic potential for tungsten. Simulation cells were thermalised to temperatures in the range from from 0.1K to 1500K. The volume of the cell was controlled by a barostat keeping the pressure fluctuating around 0 GPa. Following full thermalisation, the average of cell dimensions were monitored over 2 ns to compute the equilibrium lattice constants. The results are shown in Fig. 1.

Using the equilibrium lattice constants computed for various temperatures, we explored the simulation cells with fixed shape, size and volume containing $30 \times 30 \times 30$ unit cells. We evaluated the free energy of a perfect lattice using simulations involving 200,000 time steps. Then, we created six deformed boxes with uniaxial strains of ±0.1% in x-direction, bi-axial strains of ±0.05% in both x and y-directions, or a shear strains of ±0.1% in the xy-direction. By calculating the free energies and comparing them with the perfect lattice values, and using the expression for the elastic free energy,

$$\mathcal{F} = \mathcal{F}_0 + \frac{V}{2} C_{ijkl}\epsilon_{ij}\epsilon_{kl}, \tag{37}$$

we determined the elastic constants C_{11}, C_{12} and C_{44} in Voigt notations. The resulting values of elastic constants are shown in Fig. 2. The experimentally measured elastic constants of tungsten, plotted using the fitted functions parameterized by Lowrie *et al.* [41] are also shown for comparison. The range of experimental data extends to 1800°C.

Hexagonal or nearly circular $\frac{1}{2}\langle 111\rangle$ self-interstitial atom (SIA) dislocation loops containing 7, 19, 37 and 61 atoms were created in the initially perfect $30\times30\times30$ simulation cells. Atomic positions were determined by energy minimization through atomic relaxation performed using the conjugate gradient method, while constraining

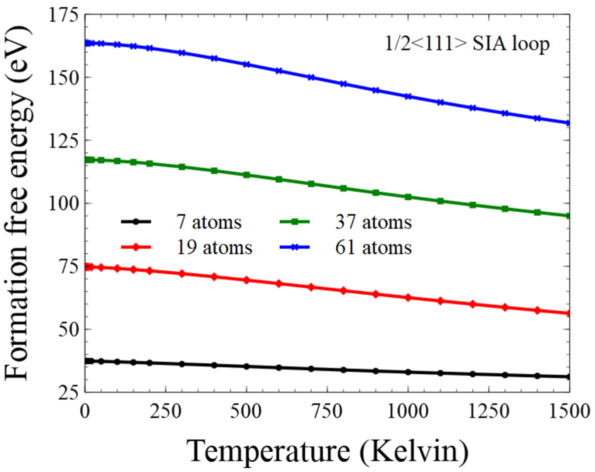

FIG. 3. Formation free energies of $\frac{1}{2}\langle 111\rangle$ SIA loops containing 7, 19, 37 and 61 atoms.

the shape and volume of the simulation cell. We evaluated the free energies of loops using the umbrella sampling and 200,000 time steps. The formation free energy was computed using the equation

$$\mathcal{F}^{form} = \mathcal{F}^{def} - \frac{N^{def}}{N^{perf}}\mathcal{F}^{perf}, \tag{38}$$

where $\mathcal{F}^{def}$ and $\mathcal{F}^{perf}$ are the free energies of configurations containing a defect and that of a perfect crystal, and N^{def} and N^{perf} are the corresponding numbers of atoms in the corresponding simulation cells. From Fig. 3 we see that all the formation free energies decrease monotonically with temperature. The data also suggest that the rate of variation of the free energy as a function of temperature is greater for the larger loops.

There are other methods for computing the free energy, for example the local harmonic approximation [42], where the free energy is evaluated from the vibration frequencies determined by diagonalizing the dynamic matrix. This effectively maps a system of interacting atoms onto a system of independent harmonic oscillators with the same number of degrees of freedom. The umbrella sampling offers an alternative way of evaluating the free energy, which appears efficient and suitable for a variety of applications [37].

A calculation of a finite-temperature elastic dipole tensor involves an element of subtlety. Larger simulation cells containing 50 × 50 × 50 unit cells are used, and the time integration involves 500,000 steps. The use of larger cell size offers an advantage by moderating fluctuations of the sum of atomic stresses. Furthermore, instead of using $\mathcal{H}^1 = \mathcal{H}_{HO}$, we choose

$$\mathcal{H}^1 = (1-\lambda)\mathcal{H}_l + \lambda\mathcal{H}_{HO} \tag{39}$$

where $\mathcal{H}_l$ is the generic lattice Hamiltonian (17) and $\lambda = 1\times 10^{-7}$ is a small constant factor. The elastic dipole tensor of a loop is calculated using equation (30). The reason for adopting the above numerical procedure is to aim to choose a small value of $\delta\mathcal{H}_{um}$. If $\delta\mathcal{H}_{um}$ is large, the exponential factor in (17) is also large, leading to large numerical errors. Besides, choosing a Hamiltonian $\mathcal{H}^1$ that is close to $\mathcal{H}^0$ implies that the phase space explored by the simulations is close to that of the original Hamiltonian, helping better quality sampling. The introduction of $\mathcal{H}_{HO}$ serves as the means for pinning the defect configuration. Fig. 4 shows how the elements of elastic dipole tensors of $\frac{1}{2}\langle 111\rangle$ SIA loops vary as functions of temperature for various loop sizes.

There is an analytical expression for P_{ij} derived in the linear elasticity approximation [8, 13, 28, 43, 44]:

$$P_{ij} = C_{ijkl}b_kA_l, \tag{40}$$

where b_k and A_l are the Cartesian components of the Burgers vector **b** and the loop vector area **A**. The loop vector area satisfies the condition [13] $V = N\Omega_0 = \mathbf{b}\cdot\mathbf{A}$, where N is the number of atoms forming the dislocation loop.

Using Eq. (40) we can evaluate the elastic dipole tensor of a loop from the finite temperature values of elastic constants and lattice constants derived from experiment [40, 41] and numerical simulations performed in this study. Fig . 5 shows the values of the matrix elements of the dipole tensor computed in this way. We see that the values are fairly similar to those derived from direct numerical calculations illustrated in Fig. 4. We note that linear elasticity ignores the dislocation core effects, which are more significant in the limit where a dislocation loop is small. According to the calculated and predicted values of P_{ij} of loops, we see that it is reasonable to use Eq. (40) derived from the continuum linear elasticity model, where the elastic constants are treated as temperature-dependent quantities.

V. CONCLUSION

We extended the concept of elastic dipole tensor to the treatment of elastic field of a defect at a finite temperature. The elastic dipole tensor is given by the volume integral of the stress field of a defect, like in the 0K case, however now the calculation requires taking the ensemble average of the integral. Examples of $\frac{1}{2}\langle 111\rangle$ SIA loops illustrate the feasibility of carrying out calculations of formation free energies and elastic dipole tensors of defects at a finite temperature. We also find that the linear elasticity formulae for the dipole tensor of loops agree well with direct numerical simulations, enabling application of finite temperature analysis to continuum level simulations.

ACKNOWLEDGMENTS

This work has been carried out within the framework of the EUROfusion Consortium and has received fund-

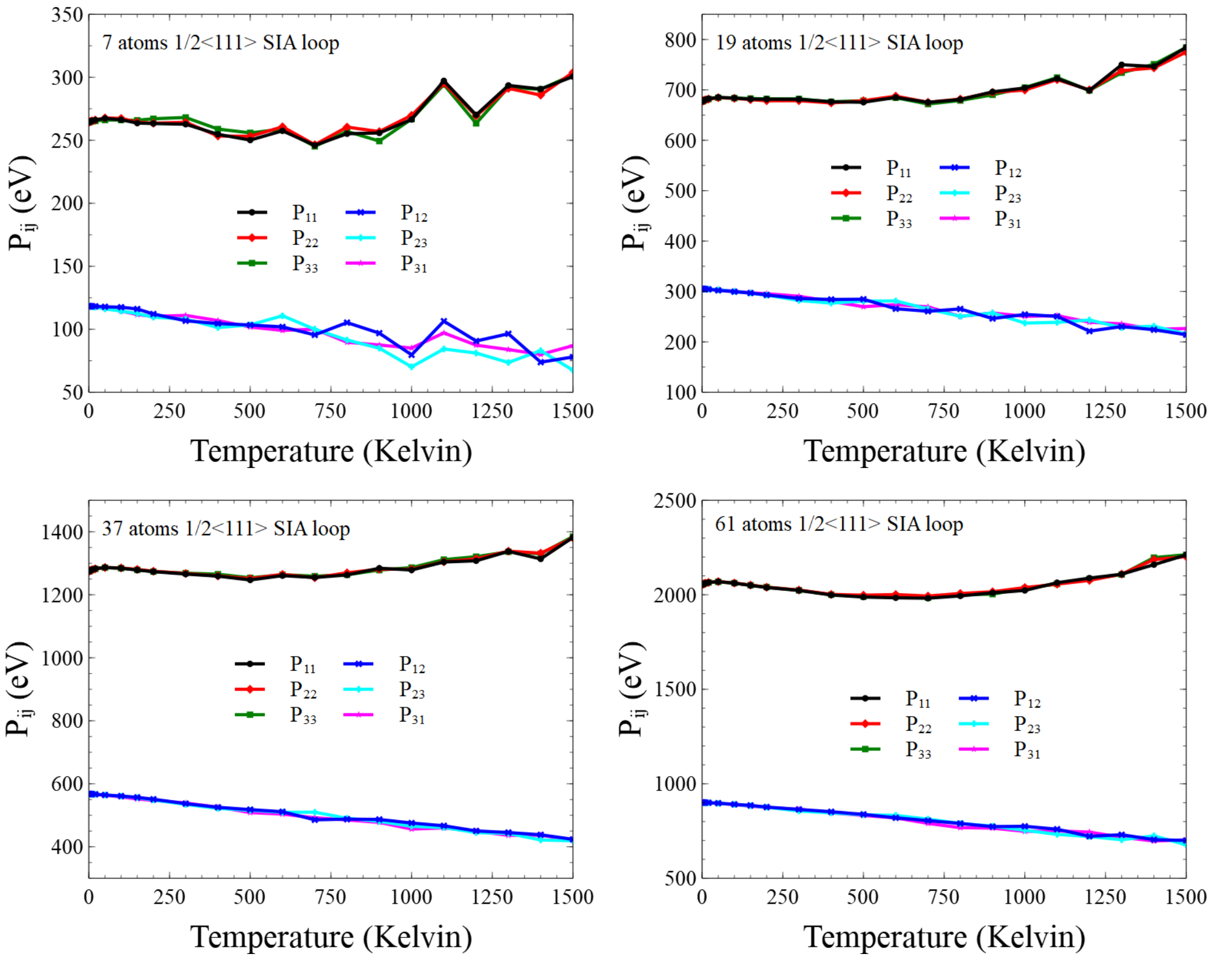

FIG. 4. Elastic dipole tensors of $\frac{1}{2}\langle 111\rangle$ self-interstitial atom dislocation loops containing 7, 19, 37 and 61 atoms calculated using umbrella sampling following Eq. (30).

ing from the Euratom research and training programmes 2014-2018 and 2019-2020 under grant agreement No. 633053 and from the RCUK Energy Programme [grant No. EP/T012250/1]. To obtain further information on the data and models underlying the paper please contact PublicationsManager@ukaea.uk. The views and opinions expressed herein do not necessarily reflect those of the European Commission. We acknowledge the use of computer resources provided by the IRIS(STFC) Consortium.

---

[1] W. Cai and W. D. Nix, *Imperfections in Crystalline Solids* (Cambridge University Press, Cambridge, England, UK, 2016).

[2] A. E. Sand, K. Nordlund, and S. L. Dudarev, Radiation damage production in massive cascades initiated by fusion neutrons in tungsten, Journal of Nuclear Materials **455**, 207 (2014), proceedings of the 16th International Conference on Fusion Reactor Materials (ICFRM-16).

[3] A. E. Sand, M. J. Aliaga, M. J. Caturla, and K. Nordlund, Surface effects and statistical laws of defects in primary radiation damage: Tungsten vs. iron, Europhysics Letters **115**, 36001 (2016).

[4] J. Byggmästar, F. Granberg, A. E. Sand, A. Pirttikoski, R. Alexander, M.-C. Marinica, and K. Nordlund, Collision cascades overlapping with self-interstitial defect clusters in Fe and W, Journal of Physics: Condensed Matter **31**, 245402 (2019).

[5] S. L. Dudarev, M. R. Gilbert, K. Arakawa, H. Mori, Z. Yao, M. L. Jenkins, and P. M. Derlet, Langevin model for real-time brownian dynamics of interacting nanodefects in irradiated metals, Phys. Rev. B **81**, 224107 (2010).

[6] S. L. Dudarev, D. R. Mason, E. Tarleton, P.-W. Ma, and A. E. Sand, A multi-scale model for stresses, strains and swelling of reactor components under irradiation, Nuclear Fusion **58**, 126002 (2018).

[7] M. Durrand-Charre, *Microstructure of Steels and Cast Irons* (Springer-Verlag, Berlin, 2003).

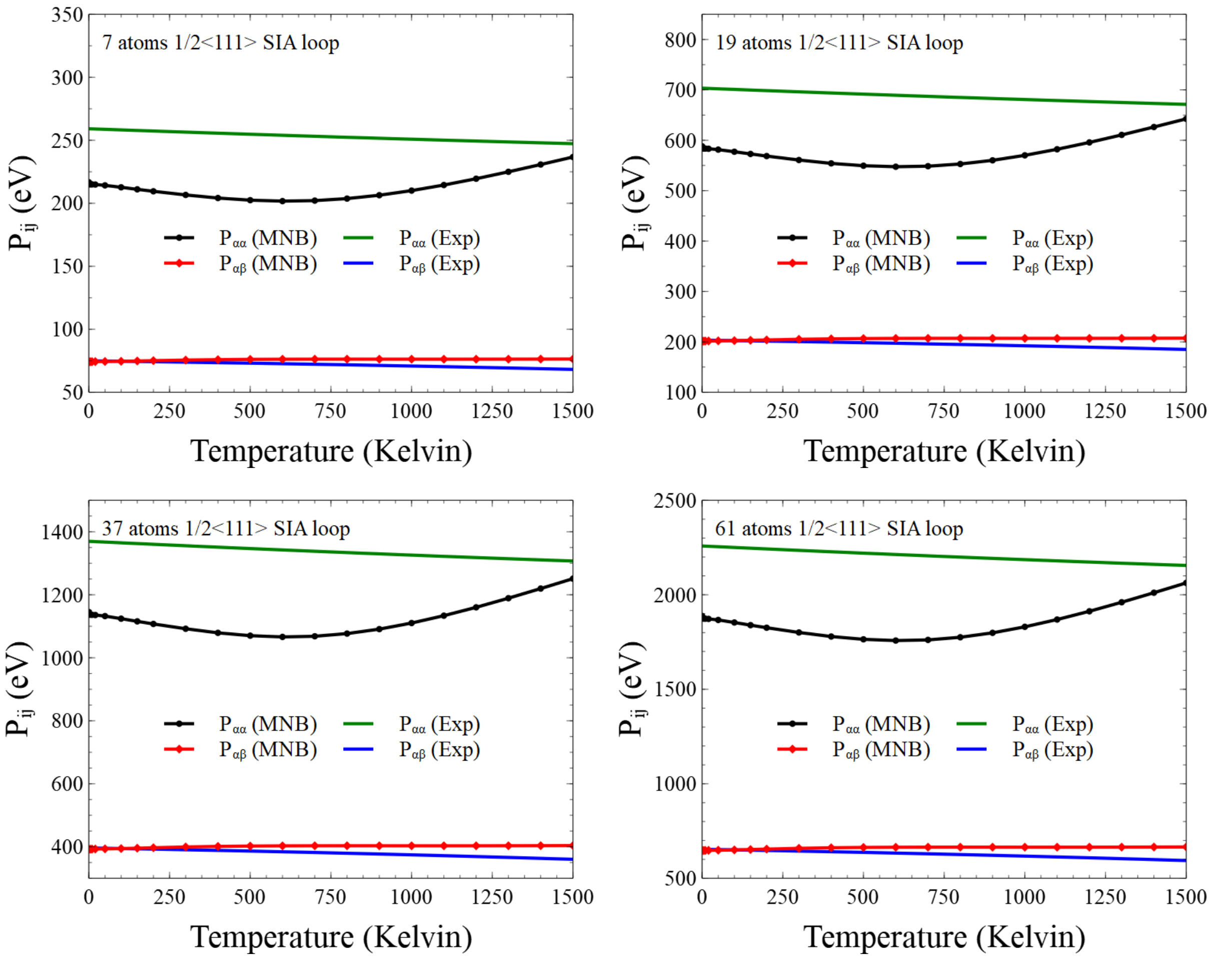

FIG. 5. Elastic dipole tensors of $\frac{1}{2}\langle 111\rangle$ SIA loops, containing 7, 19, 37 and 61 atoms, evaluated using Eq. (40) in the linear elasticity approximation. The temperature-dependent elastic constants and lattice constants are taken from experiments [40, 41] and current calculations performed using the MNB potential. $P_{\alpha\alpha}$ are the diagonal elements and $P_{\alpha\beta}$ are the off-diagonal elements of the dipole tensor.

[8] P. Dederichs, C. Lehmann, H. Schober, A. Scholz, and R. Zeller, Lattice theory of point defects, Journal of Nuclear Materials **69-70**, 176 (1978).

[9] W. Schilling, Self-interstitial atoms in metals, Journal of Nuclear Materials **69-70**, 465 (1978).

[10] E. Clouet, S. Garruchet, H. Nguyen, M. Perez, and C. S. Becquart, Dislocation interaction with C in α-Fe: A comparison between atomic simulations and elasticity theory, Acta Materialia **56**, 3450 (2008).

[11] C. Varvenne, F. Bruneval, M.-C. Marinica, and E. Clouet, Point defect modeling in materials: Coupling ab initio and elasticity approaches, Phys. Rev. B **88**, 134102 (2013).

[12] C. Varvenne and E. Clouet, Elastic dipoles of point defects from atomistic simulations, Phys. Rev. B **96**, 224103 (2017).

[13] S. L. Dudarev and P.-W. Ma, Elastic fields, dipole tensors, and interaction between self-interstitial atom defects in bcc transition metals, Phys. Rev. Materials **2**, 033602 (2018).

[14] P.-W. Ma and S. L. Dudarev, Universality of point defect structure in body-centered cubic metals, Phys. Rev. Materials **3**, 013605 (2019).

[15] P.-W. Ma and S. L. Dudarev, Effect of stress on vacancy formation and migration in body-centred-cubic metals, Physical Review Materials (2019).

[16] P.-W. Ma and S. L. Dudarev, Effect of stress on vacancy formation and migration in body-centered-cubic metals, Phys. Rev. Materials **3**, 063601 (2019).

[17] P.-W. Ma and S. Dudarev, CALANIE: Anisotropic elastic correction to the total energy, to mitigate the effect of periodic boundary conditions, Computer Physics Communications , 107130 (2019).

[18] G. Leibfried and N. Breuer, *Point Defects in Metals* (Springer, Berlin, 1978) p. 161.

[19] C. Domain and C. S. Becquart, Ab initio calculations of defects in Fe and dilute Fe–Cu alloys, Phys. Rev. B **65**, 024103 (2001).

[20] D. R. Mason, D. Nguyen-Manh, M.-C. Marinica, R. Alexander, A. E. Sand, and S. L. Dudarev, Relaxation volumes of microscopic and mesoscopic irradiation-induced defects in tungsten, Journal of Applied Physics **126**, 075112 (2019).

[21] F. Baraglia and P.-W. Ma, Dynamic model for an ensemble of interacting irradiation-induced defects in a macroscopic sample, Modelling Simul. Mater. Sci. Eng (2020).

[22] D. M. Barnett, The precise evaluation of derivatives of the anisotropic elastic Green's functions, physica status solidi (b) **49**, 741.

[23] A. Sivak, V. Chernov, V. Romanov, and P. Sivak, Kinetic monte-carlo simulation of self-point defect diffusion in dislocation elastic fields in bcc iron and vanadium, Journal of Nuclear Materials **417**, 1067 (2011), proceedings of ICFRM-14.

[24] A. Sivak, P. Sivak, V. Romanov, and V. Chernov, Energetic, crystallographic and diffusion characteristics of hydrogen isotopes in iron, Journal of Nuclear Materials **461**, 308 (2015).

[25] A. B. Sivak, P. A. Sivak, V. A. Romanov, and V. M. Chernov, Hydrogen diffusion in the elastic fields of dislocations in iron, Physics of Atomic Nuclei **79**, 1199 (2016).

[26] L. D. Landau and E. M. Lifshitz, *Theory of Elasticity*, 2nd ed. (Pergamon Press, Oxford, England, 1970).

[27] B. Puchala, M. L. Falk, and K. Garikipati, Elastic effects on relaxation volume tensor calculations, Physical Review B **77**, 174116 (2008).

[28] A. P. Sutton, *Physics of Elasticity and Crystal Defects* (Oxford University Press, Oxford, England, UK, 2020).

[29] L. D. Landau and E. M. Lifshitz, *Quantum Mechanics, Non-relativistic Theory*, 2nd ed. (Pergamon Press, Oxford, England, 1965).

[30] L. D. Landau and E. M. Lifshitz, *Mechanics*, 3rd ed. (Elsevier Butterworth-Heinemann, Oxford, England, 1976) p. 16.

[31] D. H. Tsai, The virial theorem and stress calculation in molecular dynamics, The Journal of Chemical Physics **70**, 1375 (1979), https://doi.org/10.1063/1.437577.

[32] R. J. Swenson, Comments on virial theorems for bounded systems, American Journal of Physics **51**, 940 (1983), https://doi.org/10.1119/1.13390.

[33] G. Torrie and J. Valleau, Nonphysical sampling distributions in monte carlo free-energy estimation: Umbrella sampling, Journal of Computational Physics **23**, 187 (1977).

[34] T. D. Swinburne, P.-W. Ma, and S. L. Dudarev, Low temperature diffusivity of self-interstitial defects in tungsten, New Journal of Physics **19**, 073024 (2017).

[35] K. Arakawa, M.-C. Marinica, S. Fitzgerald, L. Proville, D. Nguyen-Manh, S. L. Dudarev, P.-W. Ma, T. D. Swinburne, A. M. Goryaeva, T. Yamada, T. Amino, S. Arai, Y. Yamamoto, K. Higuchi, N. Tanaka, H. Yasuda, T. Yasuda, and H. Mori, Quantum de-trapping and transport of heavy defects in tungsten, Nature Materials **19**, 508 (2020).

[36] L. D. Landau and E. M. Lifshitz, *Statistical Physics*, 2nd ed. (Pergamon Press, Oxford, England, 1969) pp. 174–176.

[37] P.-W. Ma, S. L. Dudarev, and J. S. Wróbel, Dynamic simulation of structural phase transitions in magnetic iron, Phys. Rev. B **96**, 094418 (2017).

[38] P.-W. Ma, S. Dudarev, and C. Woo, SPILADY: A parallel CPU and GPU code for spin–lattice magnetic molecular dynamics simulations, Computer Physics Communications **207**, 350 (2016).

[39] D. R. Mason, D. Nguyen-Manh, and C. S. Becquart, An empirical potential for simulating vacancy clusters in tungsten, Journal of Physics: Condensed Matter **29**, 505501 (2017).

[40] B. N. Dutta and B. Dayal, Lattice constants and thermal expansion of palladium and tungsten up to 878°C by X-ray method, physica status solidi (b) **3**, 2253 (1963).

[41] R. Lowrie and A. M. Gonas, Single-crystal elastic properties of tungsten from 24° to 1800°C, Journal of Applied Physics **38**, 4505 (1967), https://doi.org/10.1063/1.1709158.

[42] R. LeSar, R. Najafabadi, and D. J. Srolovitz, Finite-temperature defect properties from free-energy minimization, Phys. Rev. Lett. **63**, 624 (1989).

[43] S. Dudarev and A. Sutton, Elastic interactions between nano-scale defects in irradiated materials, Acta Materialia **125**, 425 (2017).

[44] H. Trinkaus, On the investigation of small dislocation loops in cubic crystals by diffuse X-ray scattering, physica status solidi (b) **54**, 209 (1972).